CrossMark

On the equivalence of dynamically orthogonal and bi-orthogonal methods: Theory and numerical simulations

Minseok Choi [a], Themistoklis P. Sapsis [b], George Em Karniadakis [a],*

[a] *Division of Applied Mathematics, Brown University, Providence, RI 02912, USA*
[b] *Massachusetts Institute of Technology, Cambridge, MA 02139, USA*

ARTICLE INFO

ABSTRACT

The Karhunen–Lòeve (KL) decomposition provides a low-dimensional representation for random fields as it is optimal in the mean square sense. Although for many stochastic systems of practical interest, described by stochastic partial differential equations (SPDEs), solutions possess this low-dimensional character, they also have a strongly time-dependent form and to this end a fixed-in-time basis may not describe the solution in an efficient way. Motivated by this limitation of standard KL expansion, Sapsis and Lermusiaux (2009) [26] developed the dynamically orthogonal (DO) field equations which allow for the simultaneous evolution of both the spatial basis where uncertainty 'lives' but also the stochastic characteristics of uncertainty. Recently, Cheng et al. (2013) [28] introduced an alternative approach, the bi-orthogonal (BO) method, which performs the exact same tasks, i.e. it evolves the spatial basis and the stochastic characteristics of uncertainty. In the current work we examine the relation of the two approaches and we prove theoretically and illustrate numerically their equivalence, in the sense that one method is an exact reformulation of the other. We show this by deriving a linear and invertible transformation matrix described by a matrix differential equation that connects the BO and the DO solutions. We also examine a pathology of the BO equations that occurs when two eigenvalues of the solution cross, resulting in an instantaneous, infinite-speed, internal rotation of the computed spatial basis. We demonstrate that despite the instantaneous duration of the singularity this has important implications on the numerical performance of the BO approach. On the other hand, it is observed that the BO is more stable in nonlinear problems involving a relatively large number of modes. Several examples, linear and nonlinear, are presented to illustrate the DO and BO methods as well as their equivalence.

© 2014 Elsevier Inc. All rights reserved.

1. Introduction

Order-reduction schemes or reduced-order models (ROMs) have been a popular approach for the simplification and analysis of high-dimensional complex systems across many scientific and engineering disciplines. For example the stochastic framework in the analysis of fluid flows has been proven beneficial for the description of the dynamics, energy interactions, and bifurcations in unstable fluid flows [1–4], for the uncertainty quantification in CFD computations [5–8], as well as

---

* Corresponding author.
  E-mail address: george_karniadakis@brown.edu (G.E. Karniadakis).

for the development of filtering methods for turbulent systems [9–12]. Schemes based on ROMs are essentially relying on the projection of the original system into a 'suitable' set of modes representing important and essential components of the dynamics. This projection can be performed either with respect to a spatially-dependent basis or with respect to a stochastically-dependent basis. In both cases, various approaches and rules have been developed for the choice, computation, or improvement of these basis elements.

For the first family of methods (spatially-dependent basis) some of the most popular methods for the basis selection include empirical criteria such as energy-based proper orthogonal decomposition (POD) (see for example [13,14]) or more recently linear-operator-theoretic model reduction methods, such as the balanced POD [15,16]. While these have time-independent basis, a new reduced-order modeling based on approximated Lax pairs was proposed in [17] for deterministic PDEs where the basis evolves in time with applications to progressive waves or front propagation. For the second family of methods (projection to a stochastic basis) one of the most popular approaches is the Gaussian closure (assumption that the solution has a Gaussian stochastic structure) which, however, has limited applicability for problems where the non-Gaussian character is inevitable. For this case the employment of a polynomial chaos basis and its variants may provide for many cases a reliable computational scheme [18–24].

Despite the success of these methods in many problems of practical interest there are important limitations associated with them. On the one hand, methods relying on the selection of a spatial basis present important limitations in problems with strongly time-dependent character where the basis employed may become irrelevant as time evolves. Typical examples of problems belonging to this category are transient fluid flows even with a very small number of instabilities (see appendix in [25]). On the other hand, methods relying on a pre-selected stochastic structure suffer from important limitations especially in problems with highly non-Gaussian structure or with strongly transient stochastic characteristics.

Motivated by these limitations [26] followed an alternative approach for the solution of stochastic systems with high dimensionality but whose response 'lives' in a low-dimensional, possibly time-dependent, stochastic attractor. They adopt a redundant representation consisting of products of scalar, time-dependent, stochastic processes with orthonormal, deterministic, spatiotemporally-dependent fields. For both the stochastic processes and the spatially-dependent fields no particular structure is imposed and as it turns out such a representation has redundant characteristics. Nevertheless, by carefully examining the geometric properties of this representation the authors were able to illustrate the validity of a consistency condition, the *dynamical orthogonality (DO) condition*, which overcomes the redundancy of the representation and leads to independent equations for all the quantities involved. These equations (DO equations) consist of a deterministic PDE describing the evolution of the mean field, a set of deterministic PDEs describing the evolution of the spatiotemporally-dependent deterministic basis, and a set of stochastic differential equations describing the evolution of the statistical characteristics of the solution. The DO equations under appropriate constraints reproduce both the POD equations and the polynomial chaos equations. Adaptive strategies for the addition and removal of basis elements were presented in [27].

Recently, [28,29] adopted the same redundant representation used in [26] and by imposing an orthogonality condition on both the spatiotemporal and the stochastic basis (*Dynamical Bi-Orthogonality condition*) derived an independent set of equations describing the evolution of all the quantities involved (DyBO or BO equations). Although in both works the same projections were employed (with respect to physical and stochastic space) the equations rely on different conditions imposed to the representation. The aim of the current work is to examine the relationship between the two sets of equations and compare their performance through systematic numerical tests.

More specifically, the main result of this paper is the derivation of a linear, time-dependent, invertible transformation that (i) leaves the solution invariant, and (ii) transforms a BO solution to a DO solution and vice versa. Therefore, we prove that the BO set of equations is a reformulation of the DO equations. The second part of the paper is the comparison of these two formulations at the numerical level and the discussion of their relative advantages and disadvantages. The structure of the paper is as follows. In Section 2 we briefly review the DO and BO representations and their corresponding evolution equations. In Section 3, we prove the equivalence between the BO and DO along with the matrix differential equation. In order to illustrate the BO and DO and their equivalence we consider one-dimensional and two-dimensional problems: in Section 4, we consider two one-dimensional problems that are the advection and the Burgers equation, and in Section 5, we consider two two-dimensional problems including the Navier–Stokes equation. We conclude the paper with a brief summary in Section 6.

2. An overview of the BO and DO equations

We consider the following SPDE:

$$\frac{\partial u}{\partial t} = \mathcal{L}\big[u(t, x; \omega)\big], \quad x \in D, \ \omega \in \Omega \tag{1a}$$

$$u(t_0, x; \omega) = u_0(x; \omega), \quad x \in D, \ \omega \in \Omega \tag{1b}$$

$$\mathcal{B}\big[u(t, x; \omega)\big] = h(t, x; \omega), \quad x \in \partial D, \ \omega \in \Omega, \tag{1c}$$

where $\mathcal{L}$ is a differential operator, $\mathcal{B}$ is a linear differential operator, and D is a bounded domain in $\mathcal{R}^d$ where $d = 1, 2,$ or 3.

2.1. Definitions

Let $(\Omega, \mathcal{F}, P)$ be a probability space, where Ω is the sample space, $\mathcal{F}$ is the σ-algebra of subsets of Ω, and P is a probability measure. For a random field $u(x, t; \omega)$, $\omega \in \Omega$, the expectation operator of u is defined as

$$\bar{u}(x, t) \equiv E\big[u(x, t; \omega)\big] = \int_{\Omega} u(x, t; \omega) \, dP(\omega).$$

The set of all continuous and square integrable random fields, i.e., $\int_D E[u(x, t; \omega)^T u(x, t; \omega)] \, dx < \infty$, where $u(x, t; \omega)^T$ is the transpose of u, for all $t \in T$ and the bi-linear form of the covariance operator

$$C_{u(\cdot, t; \omega) v(\cdot, s; \omega)}(x, y) = E\big[\big(u(x, t; \omega) - \bar{u}(x, t)\big)^T \big(v(x, s; \omega) - \bar{v}(x, s)\big)\big], \quad x, y \in D,$$

form a Hilbert space that will be denoted by $\mathcal{H}$ [30,31]. For $u(x, t; \omega), v(x, t; \omega) \in \mathcal{H}$, the spatial inner product is defined as

$$\langle u(\cdot, t; \omega), v(\cdot, t; \omega) \rangle = \int_D u(x, t; \omega)^T v(x, t; \omega) \, dx.$$

We define the projection operator Φ_S of a field $u(x, t)$, $x \in D$ to an m-dimensional linear subspace S spanned by the orthogonal basis $S = \{w_i(x, t; \omega)\}_{i=1}^m$, $x \in D$ as follows:

$$\Phi_S\big[u(x, t; \omega)\big] = \sum_{i=1}^m \langle w_i(\cdot, t; \omega), u(\cdot, t; \omega) \rangle w_i(x, t; \omega)$$

Next, we consider the covariance operator when it acts on an element $u(x, t; \omega)$, $\omega \in \Omega$ for $s = t$:

$$C_{u(\cdot, t; \omega) v(\cdot, t; \omega)}(x, y) = E\big[\big(u(x, t; \omega) - \bar{u}(x, t)\big)^T \big(v(x, t; \omega) - \bar{v}(x, t)\big)\big], \quad x, y \in D,$$

and the integral operator, based on the covariance operator C at time t, defined by

$$K_C \phi = \int_D C_{u(\cdot, t) u(\cdot, t)}(x, y) \phi(x, t) \, dx, \quad \phi \in L^2 \tag{2}$$

is a compact, self-adjoint, and positive operator in the Hilbert space of continuous and square integrable fields L^2 equipped with inner product $\langle \cdot, \cdot \rangle$. Then the KL expansion [32] follows that every random field $u(x, t; \omega) \in \mathcal{H}$ at a given time t can be written in the form

$$u(x, t; \omega) = \bar{u}(x, t) + \sum_{i=1}^{\infty} \sqrt{\lambda_i} \phi_i(x, t) \eta_i(t; \omega), \quad \omega \in \Omega \tag{3}$$

where λ_i and $\phi_i(x, t)$ are the eigenvalues and eigenfunctions or the basis, respectively, of the following eigenvalue problem

$$\int_D C_{u(\cdot, t) u(\cdot, t)}(x, y) \phi_i(x, t) \, dx = \lambda_i \phi_i(y, t), \quad y \in D, \tag{4}$$

and ϕ_i are orthonormalized so that $\langle \phi_i, \phi_j \rangle = \delta_{ij}$ and $\eta(t; \omega)$ are zero mean, unit variance, and mutually uncorrelated, i.e. $E[\eta_i \eta_j] = \delta_{ij}$. The eigenvalues λ_i are non-negative and can be arranged in decreasing order. Then, every random field $u(x, t; \omega) \in \mathcal{H}$ can be approximated by a finite series expansion with N terms

$$u(x, t; \omega) = \bar{u}(x, t) + \sum_{i=1}^N \sqrt{\lambda_i(t)} \phi_i(x, t) \eta_i(t; \omega), \quad \omega \in \Omega. \tag{5}$$

Indeed, it is known that the KL decomposition is optimal in the mean square sense. In the context of numerical method to SPDEs, constraints are required to derive how the components in the above KL decomposition evolve in time; the components $(\lambda_i, \phi_i, \eta_i)_{i=1}^N$ are time-dependent. In the next subsections we review the two methods which have different assumptions on the constraints. For simplicity in the notation, we use the following representation in the KL decomposition

$$u(x, t; \omega) = \bar{u}(x, t) + \sum_{i=1}^N Y_i(t; \omega) u_i(x, t), \tag{6}$$

where $\sqrt{\lambda_i} \phi_i(x, t) \eta_i(t; \omega) = Y_i(t; \omega) u_i(x; \omega)$. Based on this representation we define the linear subspace $V_S = \mathrm{span}\{u_i(x, t)\}_{i=1}^N$ spanned by the basis.

2.2. Dynamically Orthogonal (DO) representation and field equations

In the DO representation, all quantities $u_i(x, t)$, $Y_i(t; \omega)$, $i = 1, \ldots, N$ are time-dependent and hence there exists some redundancy in the representation. In order to overcome this redundancy, the DO imposes the *dynamical constraint*, which dictates that the evolution of the basis $\{u_i(x, t)\}_{i=1}^N$ be *normal* to the space V_S; this can be expressed through the following condition:

$$\frac{dV_S}{dt} \perp V_S \quad \Leftrightarrow \quad \left\langle \frac{\partial u_i(x, t)}{\partial t}, u_j(x, t) \right\rangle = 0 \quad i, j = 1, \ldots, N. \tag{7}$$

This condition is referred to as the *dynamically orthogonal (DO) condition*. Note that the DO condition preserves orthonormality of the basis $\{u_i(x, t)\}_{i=1}^N$ since

$$\frac{\partial}{\partial t}\langle u_i(\cdot, t), u_j(\cdot, t) \rangle = \left\langle \frac{\partial u_i(\cdot, t)}{\partial t}, u_j(\cdot, t) \right\rangle + \left\langle u_i(\cdot, t), \frac{\partial u_j(\cdot, t)}{\partial t} \right\rangle = 0, \quad i, j = 1, \ldots, N.$$

It is proven in [26] that the DO condition leads to a set of independent and explicit evolution equations for all the unknown quantities. Next, we state the DO evolution equations without proof:

Theorem 1. *(See [26].) Under the assumptions of the DO representation, the original SPDE (1a)–(1c) is reduced to the following system of equations*

$$\frac{\partial \bar{u}(t, x)}{\partial t} = E\big[\mathcal{L}\big[u(\cdot, t; \omega)\big]\big], \tag{8a}$$

$$\frac{dY_i(t; \omega)}{dt} = \big\langle \mathcal{L}\big[u(\cdot, t; \omega)\big] - E\big[\mathcal{L}\big[u(\cdot, t; \omega)\big]\big], u_i(\cdot, t) \big\rangle, \quad i = 1, \ldots, N \tag{8b}$$

$$\sum_{i=1}^N C_{Y_i(t)Y_j(t)} \frac{\partial u_i(t, x)}{\partial t} = \prod_{V_s^\perp} E\big[\mathcal{L}\big[u(\cdot, t; \omega)\big]Y_j\big], \quad j = 1, \ldots, N, \tag{8c}$$

where the projection in the orthogonal complement of the linear subspace is defined as $\prod_{V_S^\perp} F(x) = F(x) - \prod_{V_S} F(x) = F(x) - \sum_{k=1}^N \langle F(\cdot), u_k(\cdot, t) \rangle u_k(\cdot, t)$ and the covariance of the stochastic coefficients is $C_{Y_i(t)Y_j(t)} = E[Y_i(t; \omega)Y_j(t; \omega)]$. The associated boundary conditions have the form

$$\mathcal{B}\big[\bar{u}(\xi, t; \omega)\big]\big|_{\xi \in \partial D} = E\big[h(\xi, t; \omega)\big],$$

$$\mathcal{B}\big[u_i(\xi, t)\big]\big|_{\xi \in \partial D} = E\big[Y_j(t; \omega)h(\xi, t; \omega)\big]C_{Y_i(t)Y_j(t)}^{-1},$$

and the initial conditions for the DO components are given by

$$\bar{u}(x, t_0) = E\big[u_0(x; \omega)\big],$$

$$Y_i(t_0; \omega) = \big\langle u_0(\cdot, \omega) - \bar{u}(x, t_0), v_i(\cdot) \big\rangle,$$

$$u_i(x, t_0) = v_i(x),$$

for all $i = 1, \ldots, n$, where $v_i(x)$ are the eigenfields of the covariance operator $C_{u(\cdot, t_0)u(\cdot, t_0)}$ defined by the following eigenvalue problem for $t = t_0$:

$$\int_D C_{u(\cdot, t_0)u(\cdot, t_0)}(x, y)v_i(x)\, dx = \lambda_i(t)v_i(y), \quad y \in D. \tag{9}$$

2.3. Bi-orthogonal (BO) representation and field equations

In the BO representation, the basis and stochastic coefficients are defined as follows:

$$u_i(x, t) = \sqrt{\lambda_i(t)}\phi_i(x, t), \qquad Y_i(t; \omega) = \eta_i(t; \omega), \tag{10}$$

where $\lambda_i(t)$, $\phi_i(x, t)$ and $\eta_i(t; \omega)$ are the KL components in Eq. (5). In order to overcome the aforementioned redundancy, the BO imposes the *static constraint*, which is the bi-orthogonality of the basis and stochastic coefficients in time [28]. In other words, we have the following conditions:

$$\langle u_i(\cdot, t), u_j(\cdot, t) \rangle = \lambda_i(t)\delta_{ij}, \qquad E[Y_iY_j](t) = \delta_{ij}, \quad i, j = 1, \ldots, N. \tag{11}$$

This condition is referred to as the *bi-orthogonal (BO) condition*. Note the difference between the DO and BO condition; the basis in the DO condition evolves normal to the space V_s, which maintains the basis to be orthogonal in time, while both the basis and the stochastic coefficients in the BO condition are orthogonal in time in the associated space, respectively. There is also a slight difference between the DO and BO representation; the stochastic coefficients carry the eigenvalues of the covariance operator in the DO representation while the basis carry the eigenvalues of the covariance operator in the BO representation.

Remark 1. Both the basis and the stochastic coefficients change in time while maintaining the orthogonality. Define the matrix S and M whose entries are

$$S_{ij} = \left\langle u_i, \frac{\partial u_j}{\partial t} \right\rangle, \tag{12}$$

$$M_{ij} = E\left[Y_i \frac{dY_j}{dt} \right]. \tag{13}$$

Then, by taking the derivative of the first term in Eq. (11) with respect to time, we have $\langle \frac{\partial u_i}{\partial t}, u_j \rangle + \langle u_i, \frac{\partial u_j}{\partial t} \rangle = 0$ for $i \neq j$ and $\langle \frac{\partial u_i}{\partial t}, u_i \rangle = \frac{1}{2} \frac{d\lambda_i(t)}{dt}$ for $i = j$ or $S_{ij} = -S_{ji}$ for $i \neq j$ and $S_{ii} = \frac{1}{2} \frac{d\lambda_i(t)}{dt}$. Similarly, we have $M_{ij} = -M_{ji}$ for $i \neq j$ and $M_{ii} = 0$. Note that M is skew-symmetric. It will be shown later that the matrices S and M, i.e. the rate of how the basis and the stochastic coefficients change in time, have explicit form.

Next, we present the BO evolution equations; see Appendix A for the proof and also [28].

Theorem 2. *We assume that the basis and stochastic coefficients satisfy the BO condition and there is no eigenvalue crossing. Then the original SPDE (1a)–(1c) is reduced to the following system of equations*

$$\frac{\partial \bar{u}(t,x)}{\partial t} = E\big[\mathcal{L}[u] \big], \tag{14a}$$

$$\lambda_j \frac{dY_j(t;\omega)}{dt} = -\sum_{i=1}^{N} S_{ji} Y_i + h_j, \quad j = 1, \ldots, N, \tag{14b}$$

$$\frac{\partial u_j(t,x)}{\partial t} = -\sum_{i=1}^{N} M_{ji} u_i + p_j, \quad j = 1, \ldots, N, \tag{14c}$$

where the entries for the matrix G, M and S and the vectors $\mathbf{h}$ and $\mathbf{p}$ are given as follows:

$$G_{ij} = \big\langle E\big[\mathcal{L}[u] Y_j \big], u_i \big\rangle \tag{15a}$$

$$M_{ij} = \begin{cases} \frac{G_{ij} + G_{ji}}{-\lambda_i + \lambda_j}, & \text{if } i \neq j \\ 0, & \text{if } i = j \end{cases} \tag{15b}$$

$$S_{ij} = \begin{cases} G_{ij} + \lambda_i M_{ij}, & \text{if } i \neq j \\ G_{ii}, & \text{if } i = j \end{cases} \tag{15c}$$

$$h_j = \big\langle \mathcal{L}[u] - E\big[\mathcal{L}[u] \big], u_j(\cdot, t) \big\rangle \tag{15d}$$

$$p_j = E\big[\mathcal{L}[u] Y_j \big]. \tag{15e}$$

Remark 2. The evolution equations (14a)–(14c) can be recast into matrix form with $\mathbf{u} = (u_1, \ldots, u_N)$, $\mathbf{Y} = (Y_1, \ldots, Y_N)$ and $\Lambda = \text{diag}(\lambda_1, \ldots, \lambda_N)$ as follows:

$$\frac{\partial \bar{u}(t,x)}{\partial t} = E\big[\mathcal{L}[u] \big], \tag{16a}$$

$$\frac{d\mathbf{Y}(t;\omega)}{dt} \Lambda = -\mathbf{Y}S^T + \mathbf{h}, \tag{16b}$$

$$\frac{\partial \mathbf{u}(t,x)}{\partial t} = \mathbf{u}M + \mathbf{p}, \tag{16c}$$

where S^T is the transpose of the matrix S.

We note that the rate of change of the basis and stochastic coefficients is associated with the matrix G whose entries are $G_{ij} = \langle E[\mathcal{L}[u]Y_j], u_i \rangle$, and the matrix S and M have closed form. If two eigenvalues are identical, the denominator in the non-diagonal entries of the matrix M in Eq. (15b) is singular and thus can lead to the numerical instability for the BO when two eigenvalues are getting close to each other.

The diagonal entries for S account for how the eigenvalues change in time $S_{ii} = \frac{1}{2}\frac{d\lambda_i(t)}{dt}$ as discussed in Remark 1, which can be computed exactly by Eq. (15c). This can be used as a useful adaptive criterion in the computation to decide when to add or remove modes; if the lowest eigenvalue grows quickly and is larger than a certain value, a new mode needs to be added. Another possible adaptive strategy proposed in [27] is to use as a criterion the instantaneous energy of the existing DO modes.

Remark 3. Both DO and BO representations can be viewed as an extension of KL representation in time under different assumptions. It is shown in Section 3 that they are equivalent through the invertible matrix differential equation; in other words, there is an one-to-one mapping between the BO components and DO components. However, we have observed that the BO is numerically more stable than the DO, in particular for high modes in non-linear problems. On the other hand the BO suffers from the numerical instability due to the aforementioned singularity when the eigenvalues cross while the DO does not. Examples will be presented in Sections 4 and 5 to document these statements.

3. Equivalence of BO and DO

We now prove the equivalence between the BO and DO solutions. In particular, we will prove that there is a linear transformation for the coefficients and the basis that (i) leaves the total solution invariant, and (ii) transforms the stochastic coefficients and the basis elements of the BO solution to a set of stochastic coefficients and basis elements that satisfy the DO equations. We will also show that this transformation is *invertible*, and thus it can be applied to transform the DO components to the corresponding BO components.

Based on this fact we will conclude that the two sets of equations are just a reformulation of each other since they describe the same approximate (in the sense of finite-dimensionality) solution.

Let $U = (u_1, u_2, \ldots, u_N)^T$, $\hat{U} = (\hat{u}_1, \hat{u}_2, \ldots, \hat{u}_N)^T$, $Y = (Y_1, Y_2, \ldots, Y_N)^T$ and $\hat{Y} = (\hat{Y}_1, \hat{Y}_2, \ldots, \hat{Y}_N)^T$ be the BO and the DO components, respectively. Note that $U = U(x, t)$ and $Y = Y(t; \omega)$ and the arguments x, t and ω are omitted for simplicity. We consider the linear transformation from the DO to the BO components:

$$Y = \Lambda^{-\frac{1}{2}} P \hat{Y}, \tag{17a}$$

$$U = \Lambda^{\frac{1}{2}} P \hat{U}, \tag{17b}$$

where $\Lambda = \text{diag}(\lambda_1, \ldots, \lambda_N)$ with λ_i, $i = 1, \ldots, N$ being the positive eigenvalues of the covariance operator in Eq. (11), and P satisfies the matrix differential equation

$$\frac{dP}{dt} = -\Lambda^{-\frac{1}{2}} \Sigma \Lambda^{-\frac{1}{2}} P,$$

$$P(0) = I_N, \tag{18}$$

where I_N is the $N \times N$ identity matrix, and Σ is the skew-symmetric part of the matrix S in Eq. (15c), i.e. $\Sigma_{ij} = S_{ij}$ for $i \neq j$ and $\Sigma_{ii} = 0$ for $i = 1, \ldots, N$.

We first prove the invertibility of the linear transformation through the following:

Lemma 3. *The solution $P(t)$ to the matrix differential equation (18) remains orthogonal for every time $t \geqslant 0$ given that the initial condition $P(0)$ is an orthogonal matrix. Indeed, the coefficient $F(t) \equiv -\Lambda^{-\frac{1}{2}} \Sigma \Lambda^{-\frac{1}{2}}$ of P in Eq. (18) is skew-symmetric because Σ is skew-symmetric, and thus we have*

$$\begin{aligned}
\frac{d}{dt}\left(P^T(t)P(t)\right) &= \dot{P}^T(t)P(t) + P^T(t)\dot{P}(t) \\
&= (FP)^T P + P^T FP \\
&= P^T\left(F^T + F\right)P \\
&= O_N, \quad t \geqslant 0,
\end{aligned}$$

where O_N is $N \times N$ zero matrix and the overdots denote differentiation with respect to t. Thus $\dot{P} \equiv \frac{dP}{dt}$. Therefore $P^T(t)P(t) = P^T(0)P(0) = I_N, t \geqslant 0$.

We are now ready to establish the connection between the BO and the DO components.

Theorem 4. *Suppose that U and Y satisfy the BO equations. Assume that the eigenvalues λ_i, $i = 1, \ldots, N$ of the covariance operator in Eq. (11) are discrete at any time. Then the linear transformation (17a)–(17b) defines a new set of stochastic coefficients and basis elements for which (i) $Y^T U = \hat{Y}^T \hat{U}$ the total solution remains invariant, and (ii) $\hat{U}$ satisfies the DO condition. Hence, $(\hat{U}, \hat{Y})$ is a solution of the DO equations. The invertibility of the transformation allows for the application of the theorem in the inverse direction.*

Proof. Assume that Y and U are the solutions to the BO evolution equations (14a)–(14c). Then we will prove that $\hat{Y}$ and $\hat{U}$ are the solutions to the DO evolution equations (8a)–(8c) by showing the following three properties: (i) $\hat{U}$ is an orthonormal basis, (ii) $Y^T U = \hat{Y}^T \hat{U}$, and (iii) $\hat{U}$ satisfy the DO condition and $(\hat{U}, \hat{Y})$ are DO components.

First, we define the inner product of matrix UU^T in the physical space by $\langle UU^T \rangle$ whose (i, j)-th entry is $\langle u_i, u_j \rangle$. According to the BO assumption on the basis U, we have

$$
\begin{aligned}
\Lambda &= \langle UU^T \rangle \\
&= \langle \Lambda^{\frac{1}{2}} P \hat{U} \big(\Lambda^{\frac{1}{2}} P \hat{U} \big)^T \rangle \\
&= \Lambda^{\frac{1}{2}} P \langle \hat{U} \hat{U}^T \rangle P^T \Lambda^{\frac{1}{2}}.
\end{aligned}
$$

Multiplying $P^T \Lambda^{-\frac{1}{2}}$ and $\Lambda^{-\frac{1}{2}} P$ to the left and right, respectively, on the both sides yields

$$
\begin{aligned}
\langle \hat{U} \hat{U}^T \rangle &= P^T \Lambda^{-\frac{1}{2}} \Lambda \Lambda^{-\frac{1}{2}} P \\
&= P^T P \\
&= I
\end{aligned}
$$

where we used the property of orthogonal matrix P. Hence $\hat{U}$ is an orthonormal basis.

Second, the BO and DO representations to the solution $u(x, t; \omega)$ have the same form:

$$
\begin{aligned}
u(x, t; \omega) &= \bar{u}(x, t) + \sum_{i=1}^{N} u_i(x, t) Y_i(t; \omega) \\
&= \bar{u}(x, t) + \sum_{i=1}^{N} \hat{u}_i(x, t) \hat{Y}_i(t; \omega),
\end{aligned}
$$

where $(u_i, Y_i)_{i=1}^{N}$ and $(\hat{u}_i, \hat{Y}_i)_{i=1}^{N}$ are the BO and DO components, respectively. Indeed, we obtain this directly using Eqs. (17a)–(17b)

$$
U^T Y = \big(\Lambda^{\frac{1}{2}} P \hat{U} \big)^T \Lambda^{-\frac{1}{2}} P \hat{Y} = \hat{U}^T P^T \Lambda^{\frac{1}{2}} \Lambda^{-\frac{1}{2}} P \hat{Y} = \hat{U}^T P^T P \hat{Y} = \hat{U}^T \hat{Y}.
$$

Finally, we have by the definition of the transformation

$$
U = \Lambda^{\frac{1}{2}} P \hat{U}
$$

from which we have

$$
\begin{aligned}
\dot{U} &= \frac{1}{2} \dot{\Lambda} \Lambda^{-\frac{1}{2}} P \hat{U} + \Lambda^{\frac{1}{2}} \dot{P} \hat{U} + \Lambda^{\frac{1}{2}} P \dot{\hat{U}} \\
&= (S - 2\Sigma) \Lambda^{-\frac{1}{2}} P \hat{U} + \Lambda^{\frac{1}{2}} P \dot{\hat{U}},
\end{aligned}
$$

where the second equality comes from Eq. (18) and $S = \Sigma + \frac{1}{2} \dot{\Lambda}$. We have by the definition of the matrix S as in Eq. (12)

$$
S = \langle U \dot{U}^T \rangle
$$

and putting the above two equations for U and $\dot{U}$ all together yields

$$
\begin{aligned}
S &= \langle \Lambda^{\frac{1}{2}} P \hat{U} \big((S - 2\Sigma) \Lambda^{-\frac{1}{2}} P \hat{U} + \Lambda^{\frac{1}{2}} P \dot{\hat{U}} \big)^T \rangle \\
&= \langle \Lambda^{\frac{1}{2}} P \hat{U} \hat{U}^T P^T \Lambda^{-\frac{1}{2}} (S - 2\Sigma)^T \rangle + \langle \Lambda^{\frac{1}{2}} P \hat{U} \dot{\hat{U}}^T P^T \Lambda^{\frac{1}{2}} \rangle \\
&= (S - 2\Sigma)^T + \Lambda^{\frac{1}{2}} P \langle \hat{U} \dot{\hat{U}}^T \rangle P^T \Lambda^{\frac{1}{2}}
\end{aligned}
$$

where we employed $PP^T = I$, $\langle \hat{U} \hat{U}^T \rangle = I$ to get the third equality. Hence, we have

$$
\begin{aligned}
\frac{1}{2} \Lambda^{\frac{1}{2}} P \langle \hat{U} \dot{\hat{U}}^T \rangle P^T \Lambda^{\frac{1}{2}} &= \frac{S - S^T}{2} - \Sigma \\
&= O_N
\end{aligned}
$$

Table 1
The DO and BO evolution equations. $\mathbf{u}^{DO}$ and $\mathbf{Y}^{DO}$ are the DO components of the basis and stochastic coefficients and $\mathbf{u}^{BO}$ and $\mathbf{Y}^{BO}$ are the BO components.

	DO	BO
Mean	$\frac{\partial \bar{\mathbf{u}}^{DO}}{\partial t} = E[\mathcal{L}(u)]$	$\frac{\partial \bar{\mathbf{u}}^{BO}}{\partial t} = E[\mathcal{L}(u)]$
Basis	$\frac{\partial \mathbf{u}^{DO}}{\partial t} = (\mathbf{p} - \mathbf{u}^{DO}G)C^{-1}$	$\frac{\partial \mathbf{u}^{BO}}{\partial t} = \mathbf{u}^{BO}M + \mathbf{p}$
Stochastic coefficients	$\frac{d\mathbf{Y}^{DO}}{dt} = \mathbf{h}$	$\frac{d\mathbf{Y}^{BO}}{dt} = (-\mathbf{Y}^{BO}S^T + \mathbf{h})\Lambda^{-1}$

because Σ is the skew-symmetric part of the matrix S that is exactly the first term on the right hand side and we obtain $\langle \hat{U}\hat{U}^T \rangle = O_N$ that is precisely the DO condition in vector notation. This completes the proof that $\hat{Y}$ and $\hat{U}$ are the solutions to the DO evolution equations.

The same procedure can be used to prove that if $\hat{Y}$ and $\hat{U}$ are the solutions to the DO evolution equations, then Y and U are the solutions to the BO evolution equations. $\quad\square$

In summary, the BO and DO representation come from the KL decomposition and require that both basis and stochastic coefficients are time-dependent. Hence, there exists some redundancy in the representation. In order to remove this redundancy different constraints are imposed; the DO imposes the *dynamic constraints* on the basis (called *DO condition*) from which the static connection for the basis as well as the evolution equations for the components are derived. In contrast, the BO imposes the *static constraints* on the basis and coefficients (called *BO condition*) from which the dynamic connection for the basis and coefficients as well as the evolution equations for the components are derived. However, Theorem 4 implies that both methods are equivalent in the sense that one can be derived from the other, and vice versa through the orthogonal matrix as in Eqs. (17a)–(17b). Indeed, if Eqs. (17a)–(17b) are plugged into the BO evolution equations (14a)–(14c), then the DO evolution equations (8a)–(8c) are obtained, and vice versa.

Both the evolution equations for the DO and BO are shown in Table 1, where the vector notation for the basis and stochastic coefficients are used for simplicity and coefficients in the evolution equations are defined in the previous section.

4. Numerical example: one-dimensional problems

In this section, we consider two one-dimensional problems: stochastic advection with random advection velocity and Burgers equation with random forcing.

4.1. Advection equation

Consider the following stochastic advection equation [33]

$$\frac{\partial u}{\partial t} + V(t;\omega)\frac{\partial u}{\partial x} = 0, \quad \forall (t,x) \in [0, T] \times D = [0, 2\pi] \tag{19a}$$

$$u(0, x) = g(x) = \sin(x), \quad \forall x \in D \tag{19b}$$

The randomness comes from the advection velocity $V(t;\omega)$ whose covariance kernel is given as $C_V(t_1, t_2) = \sigma \exp(-\frac{|t_1 - t_2|}{L})$, with L being the correlation length. It was shown in [33] that the stochastic advection equation (19) has exact solutions for the mean and variance.

The random transport velocity is decomposed through the truncated KL representation

$$V(t, \omega) = E[V](t) + \sum_{i=1}^{M} \sqrt{\lambda_i}\phi_i(t)Z_i, \tag{20}$$

where $\{Z_i\}_{i=1}^{M}$ are uncorrelated random variables with zero mean and unit variance, and $\{\phi_i(t), \lambda_i\}_{i=1}^{M}$ is the eigenpair corresponding to the covariance kernel $C_V(t_1, t_2)$, i.e. satisfying

$$\int_D C_V(t_1, t_2)\phi_i(t_2)\,dt_2 = \lambda_i\phi_i(t_1), \tag{21}$$

where the exponential covariance kernel has a closed form for the eigenfunctions [33]:

$$\phi_i(t) = \frac{w\cos(wt)/c + \sin(wt)}{\sqrt{(1 + w^2/c^2)T/2 + (w^2/c^2 - 1)\sin(2wT)/(4w) + (1 - \cos(2wT))/(2c)}}, \tag{22}$$

where $c = 1/L$ and $w = \sqrt{2c/\lambda_i - c^2}$. The theorem of Cameron and Martin [34] guarantees that the truncated decomposition converges to V as M goes to infinity; further, we assume that $E[V](t) = 0$.

Table 2
Dimension (or number of terms in the KL decomposition) of the parametric space with respect to energy.

Energy	Dimension (M)
95%	5
99%	18
99.9%	68

Using the DO representation, we obtain the form of the evolution operator $\mathcal{L}$

$$\mathcal{L}(u) = -V(t;\omega)\left(\frac{\partial \bar{u}}{\partial x}(x,t) + \sum_{i=1}^{N} Y_i(t;\omega)\frac{\partial u_i}{\partial x}(x,t)\right).$$

4.1.1. Numerical results for time-dependent $V(t,\omega)$

We consider the case where $V(t;\omega)$ is described by the exponential covariance in time, i.e. $C_V(t_1,t_2) = \sigma\exp(-\frac{|t_1-t_2|}{L})$ and L is the correlation length that characterizes the stochastic process. The exact solution is $u(x,t;\omega) = \sin(x - \int_0^t V(s;\omega)\,ds)$ and its mean and variance are as follows:

$$E[u](x,t) = \sin(x - \bar{V}t)\exp(-a^2\sigma^2/2) \tag{23}$$

$$V[u](x,t) = \frac{1 - \cos(2(x - \bar{V}t))\exp(-2\sigma^2 a^2)}{2} - E[u]^2, \tag{24}$$

where $\bar{V} = E[V]$ and $a = a(t)$ depends on the type of the process $V(t;\omega)$, i.e.,

$$a^2 = \begin{cases} t^2, & \text{if fully correlated,} \\ 2L(t - L(1 - \exp(-t/L))), & \text{partially correlated,} \\ t\Delta t, & \text{mutually independent} \end{cases}$$

The parameters are

$$\Delta t = 10^{-3}, \qquad L = 5, \qquad \sigma = 0.1, \qquad t_f = 5, \qquad N_s = 128.$$

We use the third-order Adams–Bashforth (AB3) as a time-integrator to minimize the error due to the time discretization. We use KL decomposition to discretize $V(t;\omega)$ and the dimension of random space is determined by how many terms in the KL decomposition we keep. Table 2 shows the dimension of the parametric space with respect to the percentage of energy above which we keep the terms. We solve the stochastic advection equation using three methods; the first two are the hybrid DO and BO methods and the other one is the probabilistic collocation method (PCM) which is one of the stochastic spectral methods along with the generalized Polynomial Chaos (gPC) [21,23,35]. As we increase the dimensionality of the parametric space by adding more terms in the KL decomposition of $V(t;\omega)$, the error of the mean and variance decreases as shown in Fig. 1. Note that, like the time-independent case, DO and PCM has the same order of magnitude of the error when they use the same parameters for numerical discretization. However, DO is much faster than PCM, especially for high-dimensional parametric space as shown in Fig. 2.

4.2. Burgers equation

In this subsection, we consider the following stochastic Burgers equation with random forcing

$$\frac{\partial u}{\partial t} + u\frac{\partial u}{\partial x} = v\frac{\partial^2 u}{\partial x^2} + \frac{1+\xi}{2}\sin(2\pi t), \quad \forall(t,x) \in [0,T] \times D = [0,2\pi]$$

$$u(0,x) = g(x), \quad \forall x \in D, \tag{25}$$

where $\xi(\omega) \in [-1,1]$ is a uniformly distributed random variable and the initial condition $g(x)$ is given as

$$g(x) = 0.5\big(\exp(\cos(x)) - 1.5\big)\sin(x + 2\pi \cdot 0.37). \tag{26}$$

We take $v = 0.05$. Note that the period of the forcing is one. Using the DO representation, we obtain the form of the evolution operator $\mathcal{L}$ and some necessary forms:

$$\mathcal{L}\big[u(x,t;\omega)\big] = -uu_x + vu_{xx} + \frac{1+\xi}{2}\sin(2\pi t)$$

$$= -\bar{u}\bar{u}_x - Y_i\frac{\partial}{\partial x}(u_i\bar{u}) - Y_iY_ju_i\frac{\partial u_j}{\partial x} + v\left(\bar{u}_{xx} + Y_i\frac{\partial^2 u_i}{\partial x^2}\right) + \frac{1+\xi}{2}\sin(2\pi t)$$
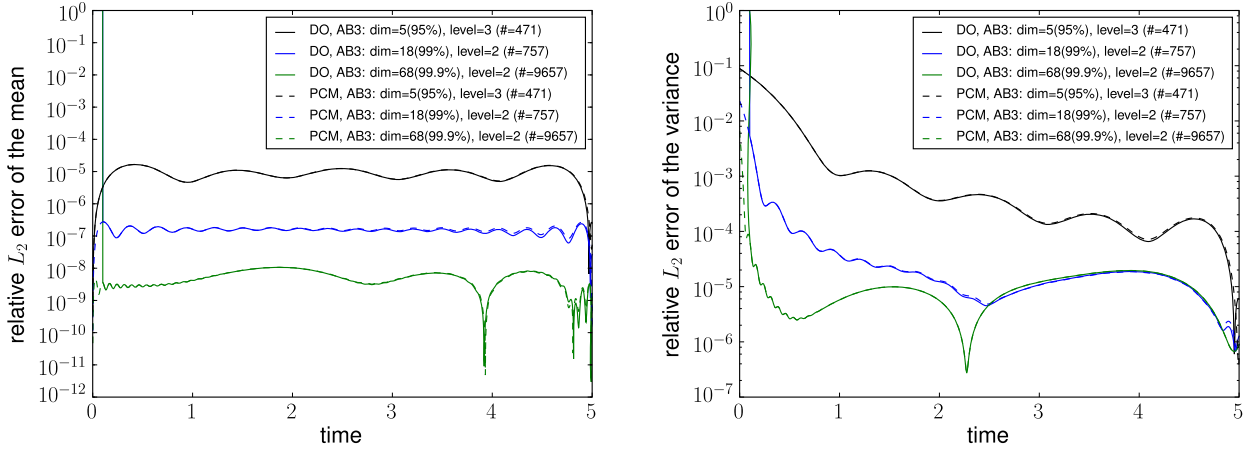
Fig. 1. Relative L_2 error for the mean (left) and variance (right). The reference solution for the mean and variance is from the exact formula. As we increase the dimension of the random space i.e. we approximate $V(t; \omega)$ better with more terms, the relative L_2 error decreases. Note that BO results do not appear in these plots but they have exactly the same accuracy as DO. (AB3 refers to the third-order Adams–Bashforth integration, and "level" refers to the level of the sparse grid.)
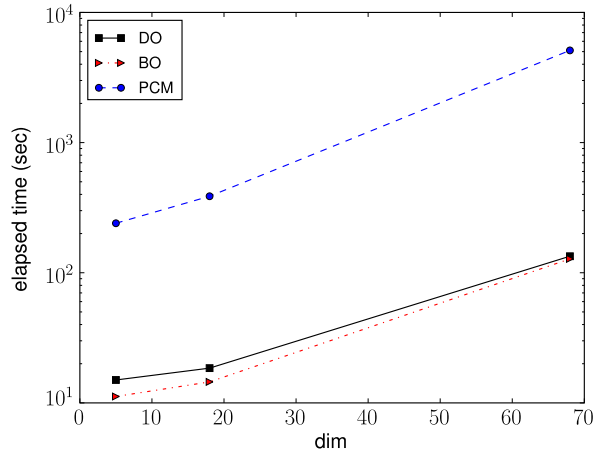

Fig. 2. Computational time on Intel Xeon X5550 2.67 GHz to solve the advection problem up to time $t = 5$ using DO, BO and PCM. DO is much faster than PCM, especially in high dimensions, and BO is slightly faster than DO for low dimensions.

$$E\big[\mathcal{L}(u)\big] = -\bar{u}\bar{u}_x - C_{ij}u_i\frac{\partial u_j}{\partial x} + \nu\bar{u}_{xx} + 0.5\sin(2\pi t)$$

$$E\big[\mathcal{L}(u)Y_j\big] = -\left(C_{ij}u_i\bar{u}_x + C_{kj}\frac{\partial u_k}{\partial x}\bar{u} + C_{ikj}u_i\frac{\partial u_k}{\partial x}\right) + \nu C_{ij}\frac{\partial^2 u_i}{\partial x^2} + E\left[\frac{\xi}{2}Y_j\right]\sin(2\pi t),$$

where $C_{ijk} = E[Y_iY_jY_k]$. Note that $E[\mathcal{L}Y_j]$ involves the third moment of the stochastic coefficients and hence the PDE for u_i is complicated. Since the initial condition is deterministic, the Y_i, $i = 1, \ldots, N$ at the initial time become zero, which makes the covariance matrix for Y_i singular. We use the *hybrid method* proposed in [8] to avoid the singularity due to the deterministic initial condition, where it starts with PCM at the beginning and switches over to DO after the stochasticity of the solution develops.

4.2.1. Computational results: hybrid DO and BO methods

We need to march for many time steps to allow the stochasticity of the system to develop fully. We have performed sensitivity studies to investigate how to choose the switching time from PC to DO but a more systematic future study is required. We can choose the number of modes at the switching time based on the eigenvalues of $C_{u(\cdot, t_s)}(x, y)$.

The parameters are as follows:

$$\Delta t = 0.001, \qquad t_s = 1, \qquad t_f = 5, \qquad N_s = 128, \qquad N_r = 64, \qquad N = 6.$$

We choose $N = 6$ because, at the switching time $t_s = 1$, the sixth mode is the largest eigenmode whose eigenvalue is larger than a pre-specified threshold value. Fourier collocation in the physical space and Legendre–Gauss collocation in the
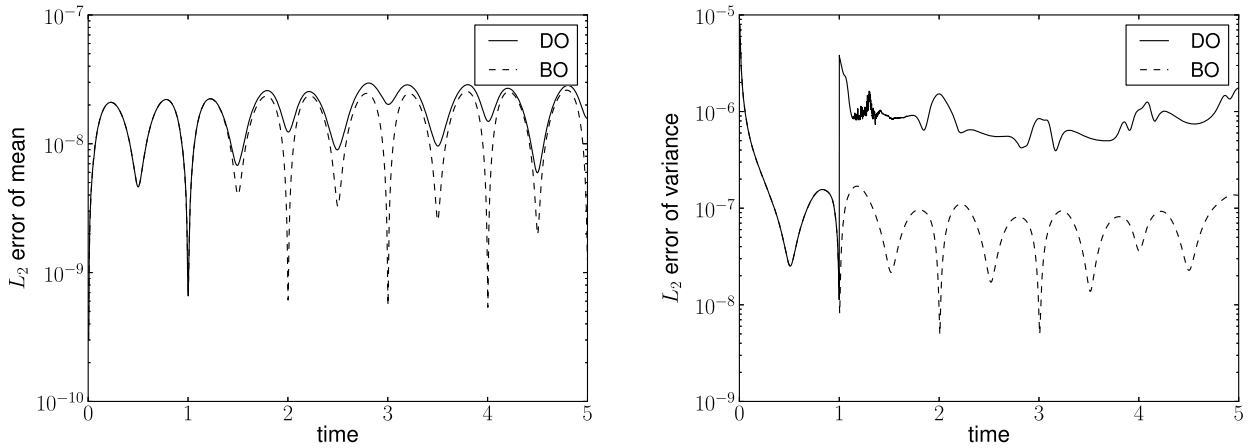
Fig. 3. Relative L_2 error for the mean (left) and variance (right) of the solution for the Burgers equation with random forcing using DO and BO with $N = 6$. Both methods have the same accuracy for the mean while BO is an order of magnitude more accurate compared to DO for the variance. BO is numerically more stable than DO for high modes while they have the same accuracy for low modes. Note that the switching time is 1 and the error before the switching time is the same as collocation method is used in the hybrid method.
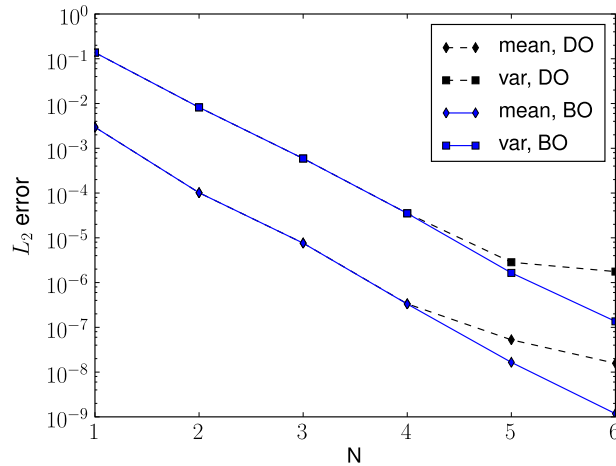
Fig. 4. Relative L_2 error for the mean and variance at $t = 5$. Exponential convergence is observed as the number of modes increases. They have the same accuracy through $N = 4$ but BO is better than DO for high modes.

parametric space are used for discretization, and third-order Adams–Bashforth (AB3) is used for a time integration. The mean and variance from the probabilistic collocation method with $N_r = 512$ using the fourth-order Runge–Kutta method are considered to be the reference solution.

The L_2 error for the mean and variance are shown in Fig. 3; BO has better accuracy in variance than DO by one order of magnitude. DO and BO are tested with different number of modes up to 6. They have the same accuracy for the first four modes but BO is better than DO for higher modes. While they are equivalent as shown in Section 3 this suggests that BO gives numerically more stable scheme than DO as shown in Fig. 4; the DO evolution equation for the basis needs an inverse of matrix whose condition number for higher number is large that may affect numerical accuracy; further research is required in order to document this point. Fig. 4 shows the exponential convergence obtained with respect to the number of modes at time $t = 5$. As mentioned above both DO and BO have the same accuracy with lower modes but BO is more accurate than DO with higher modes 5 and 6. This example is the first demonstration of the fast convergence of the DO or BO method for a nonlinear SPDE.

We now test the equivalence of DO and BO as in Section 3. From the BO evolution equations we have the BO components at every time step. Then we derive the DO components not from the DO evolution equations but from Eqs. (17a)–(17b) with P obtained from the matrix differential equation (18). The numerical integration method that preserves the orthogonality of the matrix P is employed. We compute the variance for the DO components derived from the BO components and compare this with the variances from the BO and DO. Fig. 5 shows the error in the variances of these three methods. The variance from the DO via the matrix differential equation from the BO is in between that of the BO and DO. It is worse than the BO because a first-order time integration method for the matrix differential equation is employed while a third-order time
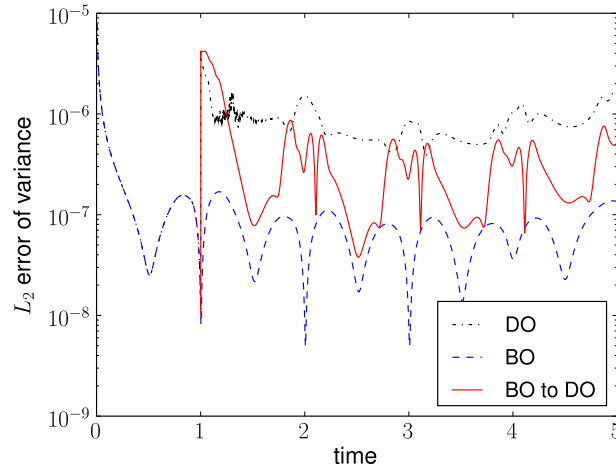
Fig. 5. Relative L_2 error for the variance at $t = 5$ with $N = 6$. The top one is the variance from the DO evolution equations; the bottom from the BO evolution equations; the middle one from the DO components via the dynamical transformation from the BO.

integration method is employed for the BO and DO. This verifies numerically the equivalence of the BO and DO in the sense that one can be obtained from the other through the matrix differential equations and vice versa.

4.2.2. Eigenvalue crossing

When the eigenvalues of the system cross each other in time, the BO evolution equations become singular because the matrix M and S in Eqs. (15b) and (15c) are singular. In this subsection we consider the Burgers equation where eigenvalues cross in time. For this we assume that the solution has an explicit form

$$u_\infty(x, t; \omega) = \xi_1(\omega)a_1(t)\cos(x - t) + \xi_2(\omega)a_2(t)\cos(2x - 3t). \tag{27}$$

The forcing term is chosen accordingly. We assume

$$a_1(t) = \sin(t), \qquad a_2(t) = \cos(3t), \tag{28}$$

and ξ_1 and ξ_2 follow the uniform distribution on $[0, 1]$. Then the exact solution for the mean and variance has an explicit form by taking the expectation on u_∞. The eigenvalues of the system are

$$\lambda_1(t) = \frac{\pi}{12}a_1^2(t), \qquad \lambda_2(t) = \frac{\pi}{12}a_2^2(t). \tag{29}$$

We assume that the boundary condition is periodic and the initial condition is given as

$$g(x) = 0.5\big(\exp\big(\cos(x)\big) - 1.5\big)\sin(x + 2\pi \cdot 0.37). \tag{30}$$

The BO and DO methods are tested with the following parameters:

$$\delta t = 10^{-4}, \qquad \nu = 0.1, \qquad t_f = 3.14, \qquad t_s = 0.01, \qquad N = 2, \qquad N_s = 128, \qquad N_r = 256, \tag{31}$$

where t_s is the switching time from polynomial chaos to DO or BO and the number of collocation points in each parametric space is 16, hence the total number comes to 256 as we have two random variables.

The eigenvalues cross each other for this example as shown in Fig. 6 and correspondingly M_{12} in Eq. (15b) jumps sharply whenever the eigenvalues cross, and this causes the numerical instability for BO.

Fig. 7 shows the L_2 error of the mean and variance for BO and DO and the numerical instability for BO arising when there is eigenvalue crossing. In order to avoid the singularity in the BO, it is proposed in [28] to freeze the stochastic coefficients temporarily and evolve only the basis when facing the eigenvalue crossing. The DO evolution equations does not suffer from the eigenvalue crossing.

5. Numerical example II: two-dimensional problems

In this section we present two-dimensional problems including Navier–Stokes problems, where the random terms come from different sources, and study the schemes described above and the equivalence of BO and DO. In the following subsections, we first study the advection–diffusion equation with random advection velocity. Then, we study Navier–Stokes equation, in particular Kovasznay flow with random velocity for a modest number of dimensions of the parametric space. The spectral/hp element method is employed in physical space [36], and PCM in parametric space. When there is a deterministic initial condition, we use the hybrid DO and BO method to avoid the singularity.
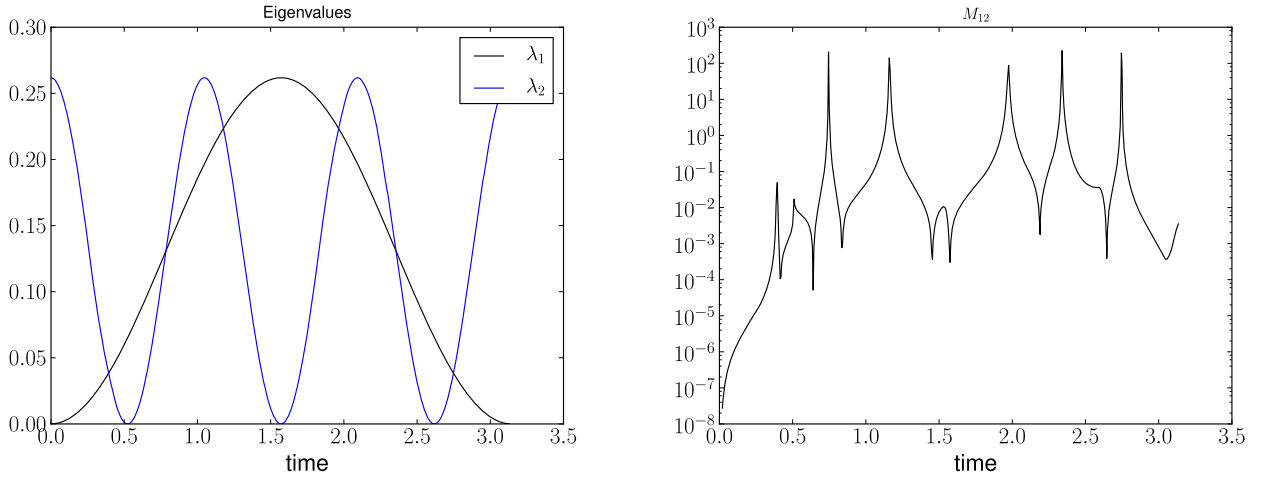
Fig. 6. Left: eigenvalues, right: M_{12}. The eigenvalues cross out at the six locations at which M_{12} peaks as shown in the right figure.
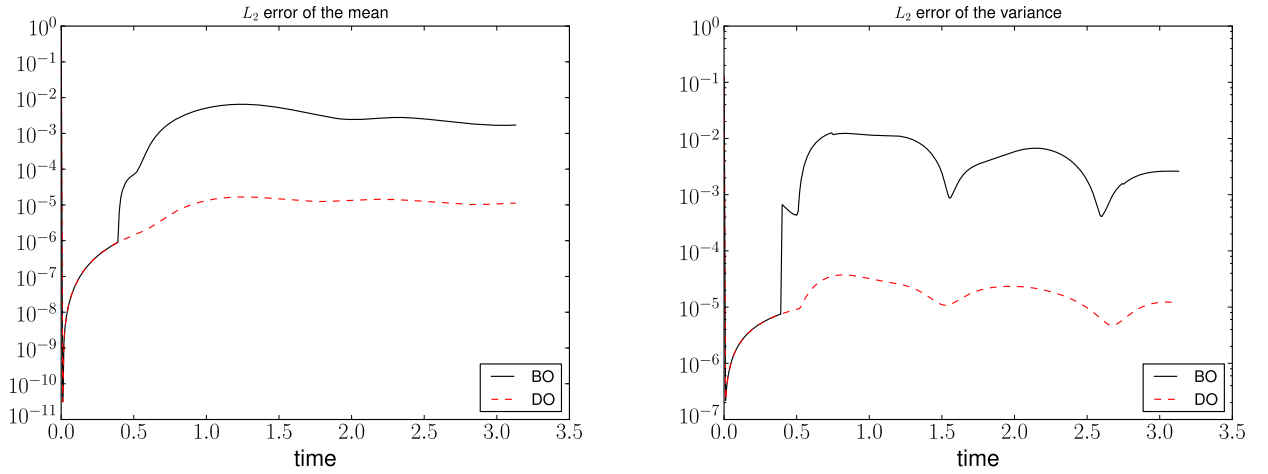

Fig. 7. Left: mean, right: variance. Both the error of the mean and variance in BO jumps when the eigenvalues cross while the error in DO does not.

5.1. Advection–diffusion equation

We consider the two-dimensional advection–diffusion equation with random advection velocity [37],

$$\frac{\partial \phi}{\partial t}(x, t; \omega) + u(x; \omega) \cdot \nabla \phi = \nu \nabla^2 \phi \quad (x, t; \omega) \in D \times [0, T] \times \Omega, \tag{32}$$

where D is a bounded domain in R^2, Ω is the sample space in the probability space, and ν is the viscosity. For this problem, we will assume deterministic boundary and initial conditions and that the advection velocity corresponds to a circular motion plus a constant random perturbation, i.e.,

$$u(x; \omega) = \big(y + a(\omega), -x - b(\omega)\big), \tag{33}$$

where $a(\omega)$ and $b(\omega)$ are random variables. The initial condition is given as

$$\phi(x, 0; \omega) = e^{-\frac{(x-x_0)^2 + (y-y_0)^2}{2\lambda^2}}, \tag{34}$$

and the corresponding exact stochastic solution is

$$\phi_e(x, t; \omega) = \frac{\lambda^2}{\lambda^2 + 2\nu t} e^{-\frac{\hat{x}^2 + \hat{y}^2}{2(\lambda^2 + 2\nu t)}}, \tag{35}$$
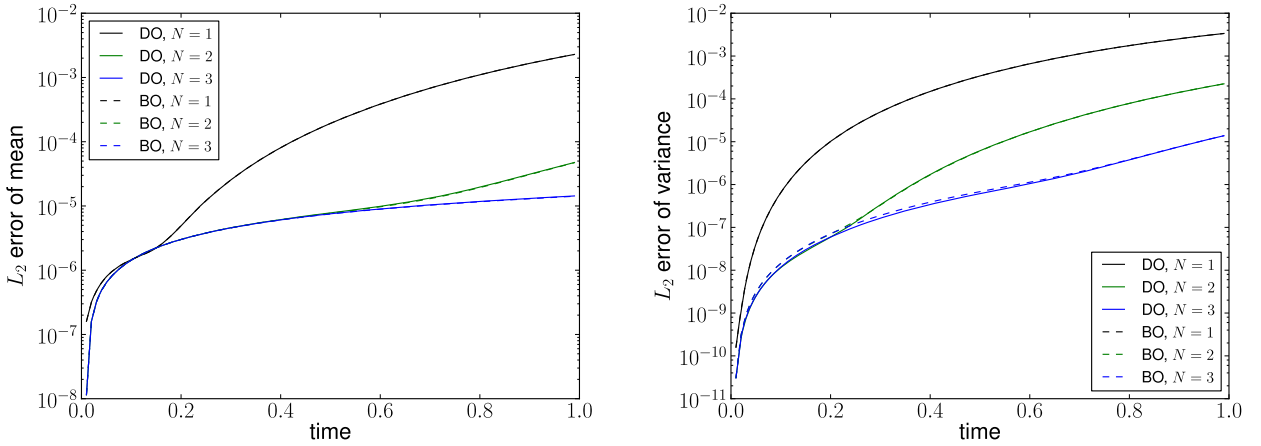
where

Fig. 8. Advection–diffusion: one-dimensional parametric space with $\xi_1 = \xi_2 = 0.1\xi$. The error of the mean (left) and variance (right) versus time with respect to different number of modes.
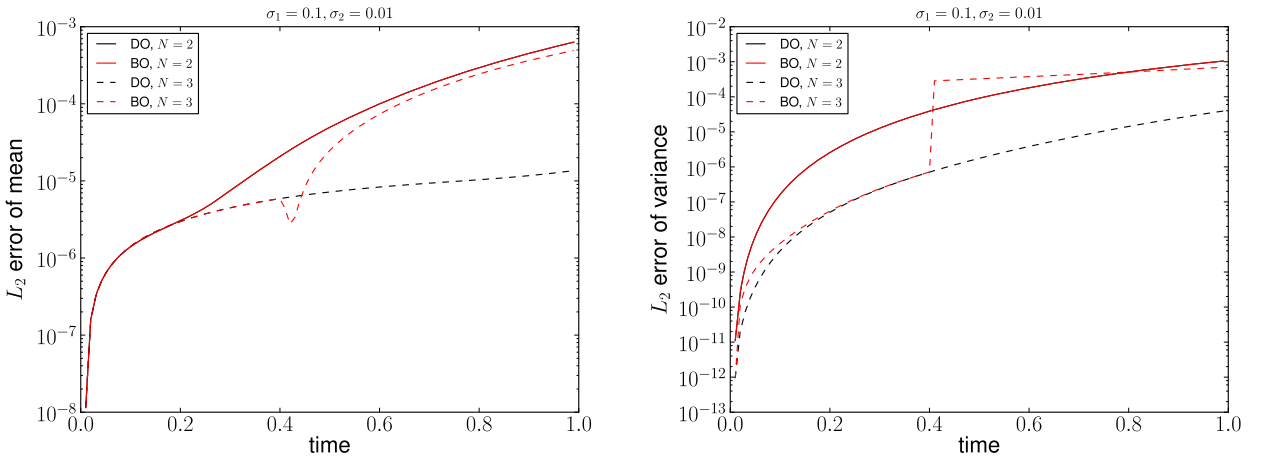

Fig. 9. Case I. The DO and BO are tested with different number of modes. As we increase the number of modes, the convergence improves. For $N = 3$, the error in the BO increases suddenly around $t = 0.4$ because of the eigenvalue crossing.

$$\hat{x} = x + b(\omega) - \big(x_0 + b(\omega)\big)\cos(t) - \big(y_0 + a(\omega)\big)\sin(t),$$
$$\hat{y} = y + a(\omega) + \big(x_0 + b(\omega)\big)\sin(t) - \big(y_0 + a(\omega)\big)\cos(t).$$

Here we set $\nu = 10^{-5}$, $\lambda = 1/8$ and $T = 1$.

Since the initial condition is deterministic, we use the hybrid method [8] for the DO and BO, i.e. start with PCM initially up to $t = t_s$ and then switch over to the DO or BO performing the KL decomposition of the solution at $t = t_s$.

First, we consider one-dimensional parametric space assuming $\xi_1 = \xi_2 = \sigma\xi$ with ξ being uniform distribution on $[-1, 1]$ and $\sigma = 0.1$. We test the BO and DO with three different number of modes. The BO and DO agree well with each other for all modes as shown in Fig. 8 and the error decreases as the modes are increased.

Next, we consider two-dimensional parametric space assuming $a(\omega) = \sigma_1\xi_1$ and $b(\omega) = \sigma_2\xi_2$ where ξ_1 and ξ_2 are two independent random variables following uniform distribution on $[-1, 1]$. We test two different sets of the variance: $(\sigma_1, \sigma_2) = (0.1, 0.01), (0.2, 0.1)$. We expect that the latter requires higher modes than the former to capture the stochastic behavior.

Case I: $(\sigma_1, \sigma_2) = (0.1, 0.01)$

The switching time is set to be $t_s = 0.01$ and two different number of modes with $N = 2, 3$ are tested. As shown in Fig. 9, the DO and BO agree well for $N = 2$ but not for $N = 3$ where the error in the BO increases suddenly around $t = 0.4$ because eigenvalue crossing occurs as shown in Fig. 10.

Case II: $(\sigma_1, \sigma_2) = (0.2, 0.1)$

We consider two different switching times: $t_s = 0.01$ and $t_s = 0.2$. When the switching time is small, then the stochasticity of the system does not evolve sufficiently so we would need a small number of modes: modes up to six are tested and as shown in Fig. 11, the DO and BO methods agree well with each other for all number of modes.
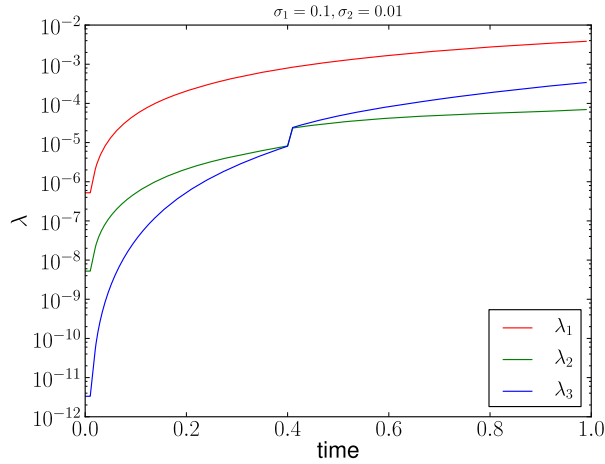
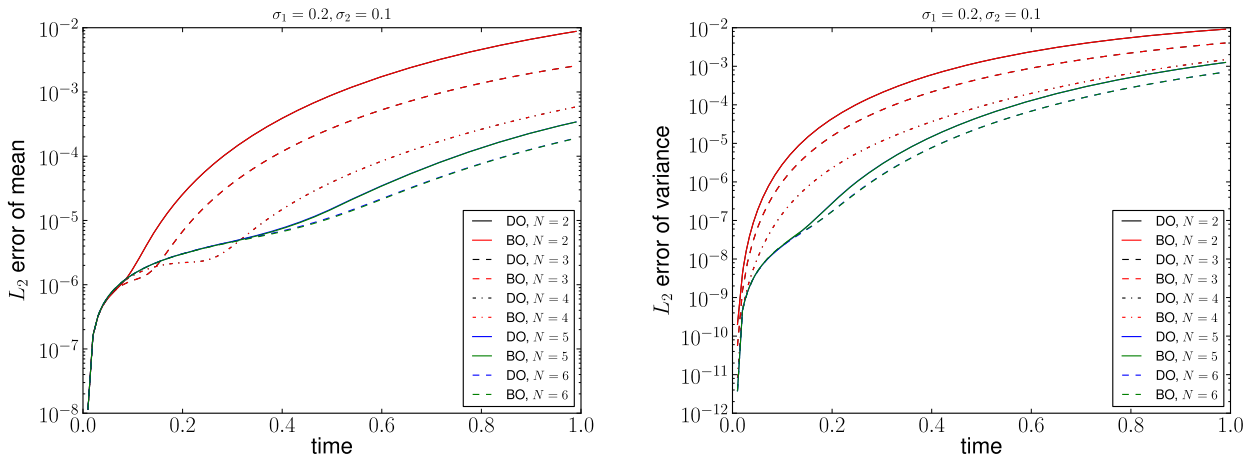**Fig. 10.** Case I. The eigenvalue crossing occurs around $t = 0.4$.

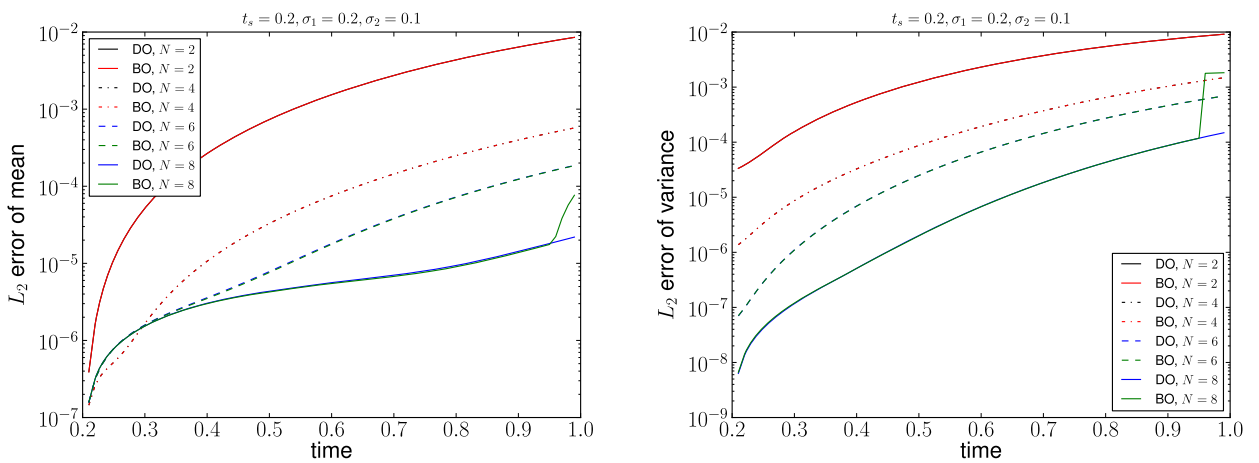**Fig. 11.** Case II with $t_s = 0.01$. L_2 error of the mean and variance.

Fig. 12. Case II with $t_s = 0.2$. L_2 error of the mean and variance.

If we switch over to BO and DO at later time $t_s = 0.2$, we need more modes to capture the stochasticity. We test up to eight modes and the DO and BO methods agree well except for $N = 8$ in Fig. 12 when the BO error increases suddenly at later time around $t = 0.95$ because of the eigenvalue crossing as shown in Fig. 13.
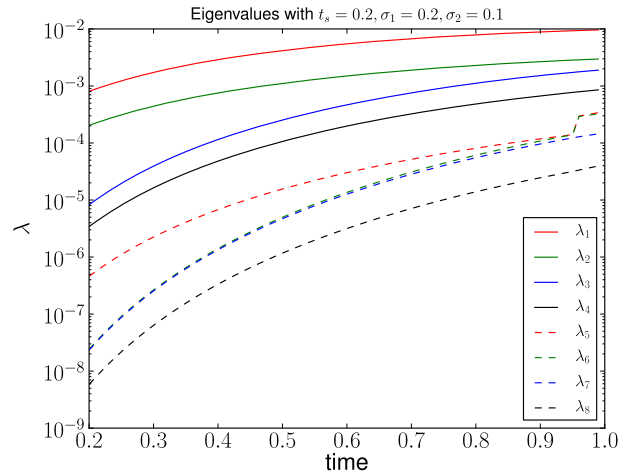
Fig. 13. Case II with $t_s = 0.2$. The eigenvalue crossing occurs around $t = 0.95$.

This example illustrates the equivalence of the BO and DO in Theorem 4 provided that any two eigenvalues are not the same. If the two eigenvalues are the same, then the BO becomes numerically unstable because of the singularity while the DO does not suffer from the singularity. This also shows that more modes are needed to have better accuracy as time goes on.

5.2. Kovasznay flow

We consider a Kovasznay flow that is a steady, laminar incompressible flow behind a two-dimensional grid

$$\frac{\partial V}{\partial t} + (V \cdot \nabla)V = -\nabla p + \nu \triangle V + F \tag{36}$$

$$\nabla \cdot V = 0 \tag{37}$$

where $V = (u, v)$, p is the pressure for a fluid with kinematic viscosity ν and F is the forcing term. The deterministic exact solution to the Navier–Stokes equations is given by

$$u = 1 - e^{\lambda x} \cos(2\pi y)$$

$$v = \frac{\lambda}{2\pi} e^{\lambda x} \sin(2\pi y)$$

$$p = \frac{1}{2}\left(1 - e^{2\lambda x}\right)$$

$$\lambda = \frac{1}{2\nu} - \left(\frac{1}{4\nu^2} + 4\pi^2\right)^{\frac{1}{2}},$$

in a rectangular domain $(x, y) \in [-0.5, 1] \times [-0.5, 1.5]$. Now we have randomness to the steady velocities that satisfy the divergence-free condition:

$$u = 1 - e^{\lambda x} \cos(2\pi y) + \sum_{m=1}^{N} \sigma_m \xi_m \cos(m\pi y) \sin(m\pi x) \tag{38}$$

$$v = \frac{\lambda}{2\pi} e^{\lambda x} \sin(2\pi y) - \sum_{m=1}^{N} \sigma_m \xi_m \sin(m\pi y) \cos(m\pi x), \tag{39}$$

where $\xi_m \in [-1, 1]$ and σ_m are independent uniformly distributed random variables and the magnitude of the randomness, respectively. Then, the forcing term $F(x, y; \omega)$ is provided accordingly so that it satisfies the Navier–Stokes equation (36).

Since this is a KL-type solution, the number of random terms N determines the number of modes in the DO and BO representation as well as the dimension of the parametric space.

Here the Reynolds number is set to $Re = 1/\nu = 40$, and 16 elements in a quadrilateral mesh are used in the prescribed domain. The polynomial order for the spectral element method in physical space is set to 10 and first-order time integration method is used. The initial conditions for the mean are assumed to be zero and those for the DO and BO components are assumed to be the exact ones to avoid the singularity. First, we consider one-dimensional parametric space, i.e. $N = 1$ to
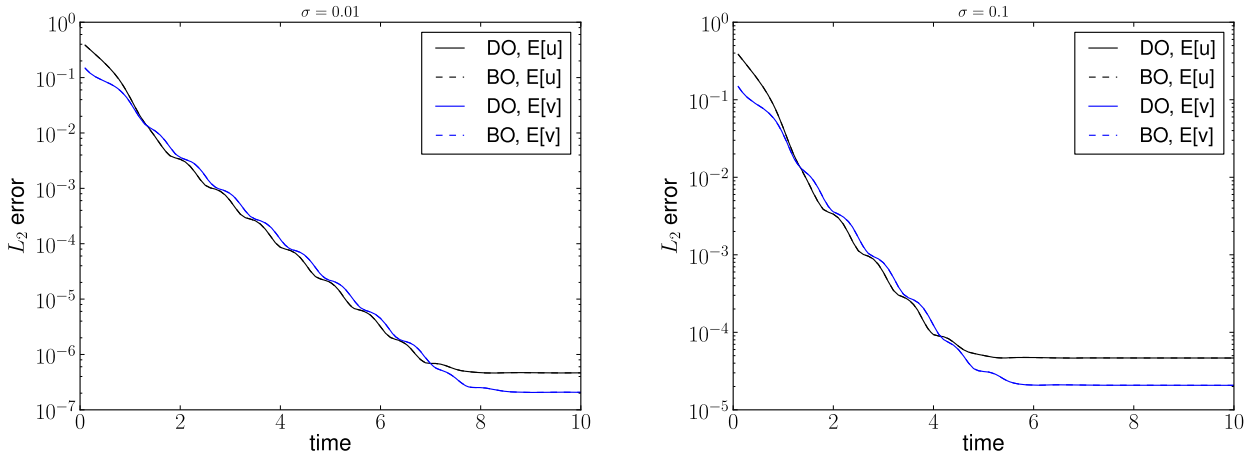
Fig. 14. L_2 error for the mean of the solution in time: $\sigma = 0.01$ (left) and $\sigma = 0.1$ (right). It converges to the steady solution after time $t = 8$ ($\sigma = 0.01$) and $t = 6$ ($\sigma = 0.1$).
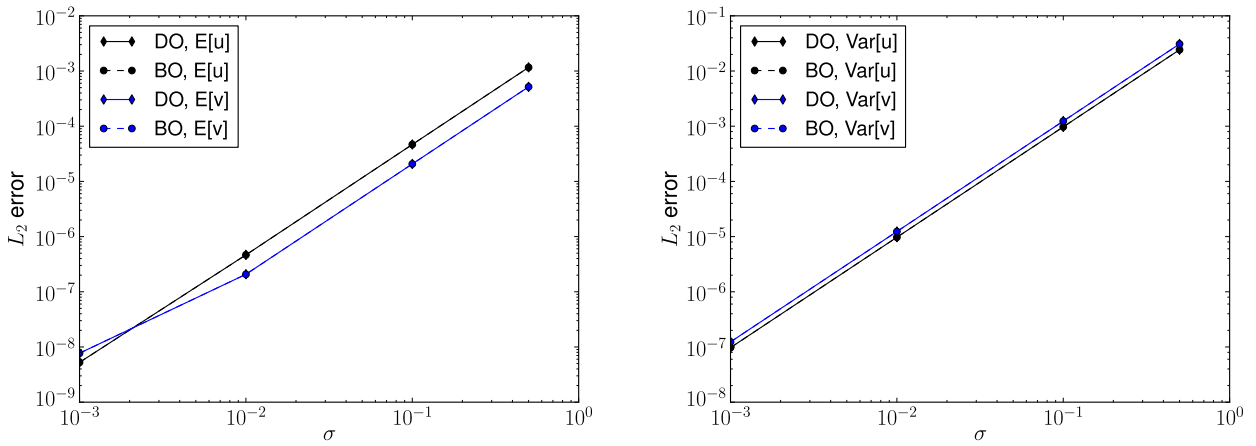

Fig. 15. L_2 error for the mean (left) and variance (right) of the steady state solution for the Kovasznay flow versus the magnitude using DO and BO.

Table 3
The magnitude σ of the random variable ξ.

$\xi \sim U[-\sigma, \sigma]$				
σ	0.5	0.1	0.01	0.001

illustrate how the DO and BO works for the two-dimensional Navier–Stokes equation. Four different values of σ are used as shown in Table 3. We solve the problem using DO and BO evolution equations.

Fig. 14 shows the L_2 error for the mean in time for the two values of σ. Fig. 15 shows the L_2 error for the mean and variance versus the magnitude σ. The L_2 error increases as the magnitude of the randomness increases. The DO and BO shows exact agreement for the mean and variance.

Next, we increase the dimension of the random space to six, i.e. Eqs. (38) and (39) have six random terms, $N = 6$. The magnitudes of the randomness are given as following: $(\sigma_1, \sigma_2, \sigma_3, \sigma_4, \sigma_5, \sigma_6) = (0.1, 0.03, 0.01, 0.003, 0.001, 0.0003)$. Similar to the one-dimensional case, the BO and DO agree well with each other as shown in Fig. 16. We have also tested ten random terms or ten dimension in the parametric space but the BO diverges due to the eigenvalue crossing while the DO converges in a similar way as in the six-dimensional case. This example shows the equivalence of the BO and DO in the Navier–Stokes problem provided that any eigenvalues are not equal to one another. If the eigenvalue crossing happens, then the BO suffers from the singularity while the DO does not.

6. Summary

In this paper, we have explored the relationship of the BO and DO method for a class of SPDEs. Both of them have time-dependent spatial and stochastic basis based on KL expansions and hence are able to track the low-dimensional structure.
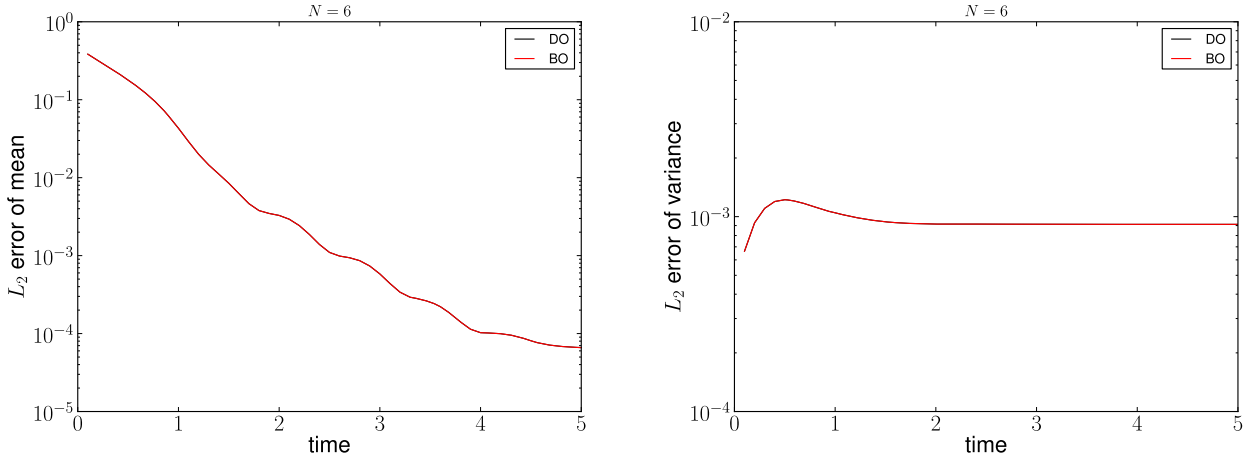
Fig. 16. L_2 error for the mean and variance in time with six dimensional parametric space.

The difference is on the assumption on how the spatial and stochastic basis evolves in time. The DO method imposes a dynamical constraint in which the evolution of the spatial basis is normal to the space spanned by the spatial basis while the BO imposes a static constraint in which the spatial and stochastic basis remain orthogonal. We have shown that the BO and DO are equivalent in the sense that the BO can be obtained dynamically through the invertible matrix differential equation and vice-versa provided that the eigenvalues are not the same.

We have applied the BO and DO for various problems including the one-dimensional advection and Burgers and two-dimensional advection–diffusion and Navier–Stokes problems. They showed that the BO and DO agree well with each other except few cases; (i) when the eigenvalue cross, then BO suffers from the singularity while DO does not, and (ii) for the Burgers problem, the DO suffers from the numerical instability when higher modes are involved. This suggests that the combination of the BO and DO might be a good idea to avoid the weak aspects of each method, which will be one of further investigations. Another future investigation will include adaptive strategies of adding and removing modes and a multiscale approach to account for some of the energy of high modes that is neglected. These issues are currently investigated and results will be reported in future publication.

Acknowledgements

Appendix A. Derivation of the BO evolution equations

In this section, we prove Theorem 2. The proof is similar to the one for the DO evolution equations in [26]. First we insert the BO representation to the SPDE (1a) to obtain

$$\frac{\partial \bar{u}}{\partial t} + \sum_{i=1}^{N} \frac{dY_i}{dt} u_i + \sum_{i=1}^{N} Y_i \frac{\partial u_i}{\partial t} = \mathcal{L}[u]. \tag{40}$$

By applying the mean value operator we obtain the first equation of the theorem (14a). By taking the inner product of the evolution equation (40) with each of the fields $\{u_j(x,t)\}_{j=1}^{N}$ we have

$$\left\langle \frac{\partial \bar{u}}{\partial t}, u_j \right\rangle + \sum_{i=1}^{N} \langle u_i, u_j \rangle \frac{dY_i}{dt} + \sum_{i=1}^{N} Y_i \left\langle \frac{\partial u_i}{\partial t}, u_j \right\rangle = \langle \mathcal{L}[u], u_j \rangle.$$

Now, we define the matrix S that has the entries $S_{ij} = \langle u_i, \frac{\partial u_j}{\partial t} \rangle$ and employ one of the BO conditions $\langle u_i, u_j \rangle = \lambda_j \delta_{ij}$ and the evolution equation for $\bar{u}$ to obtain

$$\lambda_j \frac{dY_j(t;\omega)}{dt} = -\sum_{i=1}^{N} S_{ji} Y_i + \langle \mathcal{L}[u] - E[\mathcal{L}[u]], u_j \rangle.$$

Hence, the equation for **Y** will take the final form (14b). The fact that S is equivalent to (15c) will be proved later.

We multiply Eq. (40) with Y_j and apply the mean value operator to get

$$\frac{\partial \bar{u}}{\partial t} E[Y_j] + \sum_{i=1}^{N} E\left[\frac{dY_i}{dt} Y_j\right] u_i + \sum_{i=1}^{N} E[Y_i Y_j] \frac{\partial u_i}{\partial t} = E\big[\mathcal{L}[u] Y_j\big]$$

By defining the matrix M whose entries are $M_{ij} = E[Y_i \frac{dY_j}{dt}]$ and using the BO condition we have

$$\frac{\partial u_j}{\partial t} = -\sum_{i=1}^{N} M_{ji} u_i + p_j$$

which is exactly the evolution equation (14c).

Now we prove that the two matrices S and M defined as the above are the same as those given in Eqs. (15c) and (15b), respectively. Indeed, by multiplying Y_k on the both sides in Eq. (14b) and then taking the expectation we get

$$\lambda_j M_{kj} = -\sum_{i=1}^{N} S_{ji} E[Y_i Y_k] + \big\langle E\big[\mathcal{L}[u] Y_k\big], u_j \big\rangle \tag{41}$$

where we use $E[(\mathcal{L}[u] - E[\mathcal{L}[u]]) Y_k] = E[\mathcal{L}[u] Y_k]$ because of the linearity of the expectation and $E[Y_k] = 0$. By applying the BO condition we have

$$\lambda_j M_{kj} = -S_{jk} + G_{jk}. \tag{42}$$

Interchanging the indices k and j yields

$$\lambda_k M_{jk} = -S_{kj} + G_{kj}. \tag{43}$$

This holds for $k \neq j$. For $j = k$, we have $S_{jj} = G_{jj}$ since the diagonal entries of M are zero. Summing up the last two equations and using skew-symmetric properties for S for non-diagonal elements and M yield

$$M_{jk} = \begin{cases} \frac{G_{jk}+G_{kj}}{-\lambda_j+\lambda_k}, & \text{if } j \neq k \\ 0, & \text{if } j = k \end{cases} \tag{44}$$

and substituting it back into Eq. (42) we get the explicit form for S

$$S_{jk} = \begin{cases} \frac{\lambda_k}{-\lambda_j+\lambda_k} G_{jk} + \frac{\lambda_j}{-\lambda_j+\lambda_k} G_{kj}, & \text{if } j \neq k \\ G_{jj}, & \text{if } j = k. \end{cases} \tag{45}$$

This completes the derivation.

References

[1] D. Venturi, X. Wan, G. Karniadakis, Stochastic bifurcation analysis of Rayleigh–Benard convection, J. Fluid Mech. 650 (2010) 391–413.
[2] D. Venturi, X. Wan, G. Karniadakis, Stochastic low-dimensional modelling of a random laminar wake past a circular cylinder, J. Fluid Mech. 606 (2008) 339–367.
[3] T. Sapsis, H.A. Dijkstra, Interaction of additive noise and nonlinear dynamics in the double-gyre wind-driven ocean circulation, J. Phys. Oceanogr. 43 (2013) 366–381.
[4] T. Sapsis, M. Ueckermann, P. Lermusiaux, Global analysis of Navier–Stokes and Boussinesq stochastic flows using dynamical orthogonality, J. Fluid Mech. 734 (2013) 83–113.
[5] O. Knio, O.L. Maitre, Uncertainty propagation in CFD using polynomial chaos decomposition, Fluid Dyn. Res. 38 (2006) 616–640.
[6] M. Ueckermann, P. Lermusiaux, T. Sapsis, Numerical schemes for dynamically orthogonal equations of stochastic fluid and ocean flows, J. Comput. Phys. 233 (2013) 272–294.
[7] T. Sapsis, A. Majda, Statistically accurate low order models for uncertainty quantification in turbulent dynamical systems, Proc. Natl. Acad. Sci. 110 (2013) 13705–13710.
[8] M. Choi, T. Sapsis, G.E. Karniadakis, A convergence study for SPDEs using combined polynomial chaos and dynamically-orthogonal condition, J. Comput. Phys. 245 (2013) 281–301.
[9] A.J. Majda, J. Harlim, Filtering Complex Turbulent Systems, Cambridge University Press, 2012.
[10] A. Bain, D. Crisan, Fundamentals of Stochastic Filtering, Stochastic Modeling and Applied Probability, Springer, New York, 2009.
[11] P.F.J. Lermusiaux, Uncertainty estimation and prediction for interdisciplinary ocean dynamics, J. Comput. Phys. 217 (2006) 176–199.
[12] A. Majda, D. Qi, T. Sapsis, Blended particle filters for large dimensional chaotic dynamical systems, Proc. Natl. Acad. Sci. (2014), in press.
[13] L. Sirovich, Turbulence and the dynamics of coherent structures, parts I, II and III, Q. Appl. Math. XLV (1987) 561–590.
[14] P. Holmes, J. Lumley, G. Berkooz, Turbulence, Coherent Structures, Dynamical Systems and Symmetry, Cambridge University Press, 1996.
[15] S. Lall, J.E. Marsden, S. Glavaski, A subspace approach to balanced truncation for model reduction of nonlinear control systems, Int. J. Robust Nonlinear Control 12 (2002) 519.
[16] Z. Ma, C.W. Rowley, G. Tadmor, Snapshot-based balanced truncation for linear time-periodic systems, IEEE Trans. Autom. Control 55 (2010) 469.
[17] J.-F. Gerbeau, D. Lombardi, Reduced-order modeling based on approximated lax pairs, arXiv:1211.4153.
[18] R. Ghanem, P. Spanos, Stochastic Finite Elements: A Spectral Approach, Springer-Verlag, 1991.

[19] D. Xiu, G.E. Karniadakis, The Wiener–Askey polynomial chaos for stochastic differential equations, SIAM J. Sci. Comput. 24 (2002) 619–644.
[20] D. Xiu, G.E. Karniadakis, Modeling uncertainty in flow simulations via generalized polynomial chaos, J. Comput. Phys. 187 (2003) 137–167.
[21] D. Xiu, J. Hesthaven, High order collocation methods for differential equations with random inputs, SIAM J. Sci. Comput. 27 (3) (2005) 1118–1139.
[22] X. Wan, G.E. Karniadakis, An adaptive multi-element generalized polynomial chaos method for stochastic differential equations, J. Comput. Phys. 209 (2005) 617–642.
[23] I. Babuska, F. Nobile, R. Tempone, A sparse grid stochastic collocation method for partial differential equations with random input data, SIAM J. Numer. Anal. 46 (2008) 2309–2345.
[24] J. Foo, X. Wan, G.E. Karniadakis, The multi-element probabilistic collocation method: error analysis and simulation, J. Comput. Phys. 227 (2008) 9572–9595.
[25] T.P. Sapsis, Attractor local dimensionality, nonlinear energy transfers, and finite-time instabilities in unstable dynamical systems with applications to 2D fluid flows, Proc. R. Soc. A 469 (2153) (2013) 20120550.
[26] T. Sapsis, P. Lermusiaux, Dynamically orthogonal field equations for continuous stochastic dynamical systems, Physica D 238 (2009) 2347–2360.
[27] T.P. Sapsis, P.F.J. Lermusiaux, Dynamical criteria for the evolution of the stochastic dimensionality in flows with uncertainty, Physica D 241 (2012) 60.
[28] M. Cheng, T. Hou, Z. Zhang, A dynamically bi-orthogonal method for time-dependent stochastic PDES I: Derivation and algorithms, J. Comput. Phys. 242 (2013) 843–868.
[29] M. Cheng, T. Hou, Z. Zhang, A dynamically bi-orthogonal method for time-dependent stochastic PDES II: Adaptivity and generalizations, J. Comput. Phys. 242 (2013) 753–776.
[30] K. Sobczyk, Stochastic Wave Propagation, Elsevier Publishing Company, 1985.
[31] Y. Rozanov, Random Fields and Stochastic Partial Differential Equations, Kluwer Academic Press, 1996.
[32] M. Loeve, Probabilistic Theory II, Springer-Verlag, 1978.
[33] M. Jardak, C.-H. Su, G.E. Karniadakis, Spectral polynomial chaos solutions of the stochastic advection equation, J. Sci. Comput. 17 (2002) 319–338.
[34] R.H. Cameron, W.T. Martin, The orthogonal development of non-linear functionals in series of Fourier–Hermite functionals, Ann. Math. 48 (2) (1947) 385–392.
[35] J. Foo, G.E. Karniadakis, Multi-element probabilistic collocation in high dimensions, J. Comput. Phys. 229 (2009) 1536–1557.
[36] G.E. Karniadakis, S.J. Sherwin, Spectral/hp Element Methods for Computational Fluid Dynamics, second edition, Oxford University Press, 2005.
[37] X. Wan, D. Xiu, G.E. Karniadakis, Stochastic solutions for the two-dimensional advection–diffusion equation, SIAM J. Sci. Comput. 26 (2004) 578–590.